Advance Sustainable Science, Engineering and Technology (ASSET)
Vol. 6, No.4, October 2024, pp. 02404019-01 ~ 02404019-011
ISSN: 2715-4211 DOI: https://doi.org/10.26877/asset.v6i4.1002

Advances in Deep Learning for Skin Cancer Diagnosis

Maysaa R. Naeemah[1,2], Mohammed Y. Kamil[2*]

[1]College of Science for Women, Baghdad University, Baghdad, Iraq

[2]College of Science, Mustansiriyah University, Baghdad, Iraq

*m80y98@uomustansiriyah.edu.iq

Abstract. The most prevalent type of cancer worldwide is known as skin cancer. Early detection is critical because if left undiagnosed in the primary stage, it might be fatal. Although there are differences within the class and high inter-class similarities, it is too difficult to distinguish with the naked eye. Owing to the disease's global prevalence, a number of deep learning based automated systems were created thus far to help doctors identify skin lesions early on. Using pre-trained ImageNet weights and fine-tuning the Convolutional Neural Networks (CNNs), we trained VGG19 on the HAM10000 dataset. The optimal performance was observed with FT. The model that was created, which yielded an accuracy that was greater overall than the one used in transfer learning, was 82.4±1.9 %. By offering a second opinion and supporting the clinician's diagnosis, this performance could lower morbidity and treatment costs.

Keywords: Skin cancer, Deep learning, Transfer learning, Convolutional Neural Network, Fine-tuning, Image Classification, Medical Imaging, Dermatology, AI in Healthcare

(Received 2024-08-26, Accepted 2024-10-02, Available Online by 2024-10-17)

1. Introduction

Skin cancer is a pathological state characterized by the excessive proliferation of skin cells, mostly caused by DNA mutations or genetic abnormalities. The primary factor contributing to this anomaly is prolonged exposure to UV light emitted by the sun [1]. Other variables contribute to an increased susceptibility to skin cancer, such as the use of alcoholic beverages, being overweight, experiencing sunburns, exposure to radiation, having a family history of the disease, possessing compromised immune systems, and genetic diseases [2-4]. DL techniques, particularly Convolutional CNNs, have emerged as the preferred paradigm in different medical image applications. It has been observed that deep convolutional neural networks (DCNNs) efficiently integrate low-, middle-, and high-level features throughout the network prior to forwarding them to fully connected neural networks [5, 6]. More recently the deep convolutional networks showed that the training of deeper recognition models could result in producing a higher level of accuracy in cases where convolutional networks include connections from the input to the output across all of the layers [7, 8].

T. Emara et al. (2019) instead of utilizing various complex models, have recommended one Inception-v4 model that has been modified for the classification of data that has been extracted from the dataset. Utilizing feature reuse more specifically, adding long residual connections enhanced the proposed model's efficiency. This included joining high-level layers with features that had been gathered

from the earlier layers, which resulted in the improvement of the classification performance of the model. In the case of being tested on a testing set, the accuracy of the proposed architecture has been 94.70% [2]. Z. Qin et al. (2020), have improved the established skin lesion classification performance by utilizing Generative Adversarial Network (GAN) -based data augmentation technique. The basic style-based GAN model was followed in the proposal for skin lesion style-based GAN types. Regarding image classification, a transfer learning approach was used to build the classifier on top of a pre-trained deep neural network. Ultimately, the training set was expanded to include synthetic images from proposed skin lesion style-based GANs to aid in training the classifier for improved performance of the classification. The primary classification indicators, such as sensitivity, accuracy, specificity, balanced multiclass accuracy, and average precision, have been 83.20%, 95.2%, 74.30%, 83.10%, and 96.60% on the International Skin Imaging Collaboration (ISIC) 2018 Challenge after the addition of synthesized images have been added to training dataset [9]. A. Mahbod et al. (2020) utilized pre-trained CNN and Transfer Learning (TL) approaches, for the examination of image size impacts on skin lesion classification. Cropping and scaling operations had been implemented on the dermoscopic images that were obtained from ISIC skin lesion classification challenge data-sets. This produced six distinct sizes, ranging from 224 x 224 to 450 x 450. The efficiency of classifying 3 broadly accepted CNNs, which are EfficientNet-B1, EfficientNet-B0, and SeReNeXt50-has been researched. Also, they published a concept and assessed a fusion approach which is referred to as the multi-scale multi-CNN(MSM-CNN). This study's technique has been created around a 3-leveled ensemble strategy that utilizes 3 distinct network designs. Different-sized cropped dermoscopic images have been utilized for the training of such design. The conclusions of their research have shown that, compared with image re-sizing, utilizing image cropping as a technique produced better results for classification performance. This benefit has been viewed at each image scale that has been looked at. On the ISIC 2018 skin lesion classification challenge test set, the MSM-CNN system showed balanced multi-class accuracy [10]. M. S. Ali et al. (2021) have presented a cutting-edge deep convolutional neural network (DCNN) model that was successful in highly accurate classification of benign and malignant skin lesions. For the removal of noise and artifacts present in the input images, the researchers initially utilized a kernel or filter throughout the phase of pre-processing. After that, they went on and normalized input images and extracted the relevant features which help with accurate data classification. Finally, the researchers have increased image quantity by the use of the approaches of data augmentation, which have enhanced the accuracy of the classification rate. The researchers carried out comparison analyses using some TL models, like ResNet, MobileNet, VGG-16, AlexNet, DenseNet, and others, for the evaluation of their proposed DCNN model. Maximak reported values have been 93.16% and 91.93% for training and testing accuracies, respectively [11]. I. Iqbal et al. (2021) have created a DCNN model with several layers and various sizes of filters. To enhance its performance and efficiency, it has been enhanced to have a smaller number of filters and parameters. (ISIC-18, -17, and -19) data have been utilized in experimentations for the creation of dermoscopic images. Using some of the criteria like sensitivity, specificity, accuracy, and others, experimental results of the suggested DCNN approach have been illustrated. Concerning the ISIC-17 dataset, the model has exhibited 94% accuracy, 93% sensitivity, and 91% specificity. Experimental results have shown that the proposed DCNN approach performed better than the current algorithms. Particularly, it classified the skin lesions in the ISIC17 with an area under the receiver operating characteristics of 0.964 [12]. M. A. Khan et al. (2021) proposed the CNN architecture, specifically MASK R-CNN, was built. The base architecture was provided by the Resnet50 model and the feature pyramid network (FPN). The mapping regarding the features depending on fully connected layers was necessary to build the final mask. An architecture of a CNN with 24 layers was created throughout the classification stage. Activation mechanisms in such architecture are dependent upon the manifestation of higher-level features. To perform the final classification, the best features of CNN were finally employed and incorporated into soft max classifiers. To validate the segmentation process, three datasets PH2, ISBI2016, and ISIC2017 were used. In contrast, the classification made use of the HAM10000 dataset. The aforementioned features, namely precision 87.01%, sensitivity 85.57%,

accuracy 86.5%, and F1-Score 86.28%, indicate that the proposed technique performs better than other well-established methods [13].

In the presented study, we suggest a skin lesion classification system depending on deep neural networks. Our dataset, HAM10000, included seven different types of skin lesions. To fit the training model's input size, we first resized the images. The high data imbalance problem was solved which affects the multi-class classification task. To enable the models to produce accurate predictions, we added at least one label to that data to characterize its context. Input images have been normalized to a standard range within (0, 1). A significant amount of training data is necessary for DL classification networks to be trained appropriately to overcome such issues; we augmented the training data. To get the optimum outcome, the models have been trained using different combinations of hyper-parameters. VGG19 model was employed; it is trained via FT and TL. Lastly, five criteria were used to assess the classification models' performance.

2. **Methods**

This section provides a detailed description of all the materials and techniques we utilized to construct the suggested system, such as model training, data preparation, and pre-trained models.

2.1. VGG19

A variation of the VGG model depending on the design of VGG16 is called VGG19 [14]. The depth of the architecture is the primary distinction. It has 19 layers—3 fully connected layers, 16 convolution layers, 5 maxpool layers, and 1 softmax layer—but it adheres to the same basic pattern of convolution as well as maxpool blocks as VGG16 [15].

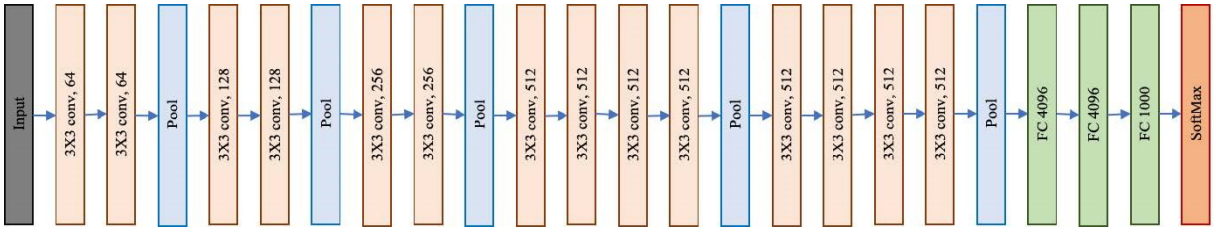

Figure 1. VGG19 Architecture [16]

2.2. Datasets

The dataset used for this research is the HAM10000 ("Human Against Machine with 10015 images"). This dataset has been provided by the ISIC 2018 classification challenge, which is why, it is referred to as the ISIC 2018 dataset as well. There are seven types of skin lesions in HAM each of the one categories has been listed in Table 1.

Table 1. Dataset distribution

Diagnostic category	Symbol	No. of images	Ratio
Actinic Keratosis and Intraepithelial Carcinoma	AKIEC	327	3.27%
Basal Cell Carcinoma	BCC	514	5.13%
Benign Keratosis	BKL	1099	10.97%
Dermatofibroma	DF	115	1.15%
Melanoma	MEL	1113	11.11%
Melanocytic Nevi	NV	6705	66.95%
Vascular Lesion	VASC	142	1.42%

Those 7 detailed diagnostic classes cover over 95% of the types of skin lesions. There are noticeable differences within one class, whereas inter-class similarity can be rather large. Additionally, it's a dataset with unbalanced classes, where over 2/3 of the images belong to the melanocytic nevi whereas the dermatofibroma is only responsible for 1.15% by contrast. Concerning image quality, those images have various conditions of lighting and perspective. This is why, it can be considered as a substantial challenge for the classifier to differentiate those 7 classes, and sample images of every class have been depicted in Figure 2. The dataset is freely available through the Kaggle repository.[17]

2.3. Pre-processing

When using DL, data pre-processing significantly affects the diagnosis of skin diseases. The most popular kind of pre-processing approach, image resizing, was one of the actions done in this research. As required by the models, we scaled every image in the dataset from 450 × 600 RGB to 224 × 224. In the case when creating a model, data labeling, sometimes called data annotation, is part of the preprocessing step. Each class now has at least one label added to complete that task. Table 1 provides proof of the extreme class imbalance present in the final dataset, which will introduce severe bias to the system's performance. Data imbalance represents one of the data limitations affecting DL model performance. In some specific cases, the number of training instances in one category is much higher compared to it in another. The model has few opportunities to learn about minority classes, and the training is skewed as opposed majority. As a result, this model keeps identifying all the input as being part of the majority class and fails to treat data that belongs to the minority class adequately. And solve this problem, the data was balanced by making 500 samples for each class of the data set. After that, original images go through a process of normalization. To avoid problems at the training time, the criterion that has been utilized is division 1 between the maximum pixel value, for 1/255 case, which gives values ranging between 0 and 1.

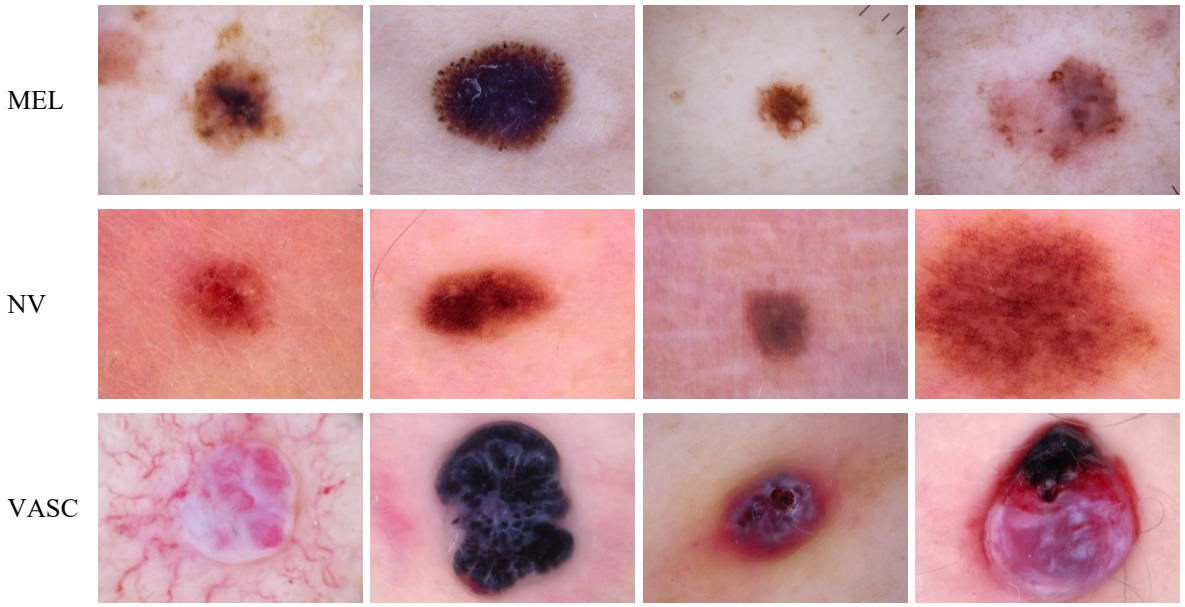

Figure 2. Sample images from the dataset

2.4. Data augmentation

A significant amount of training data is necessary for DL classification networks to be trained appropriately. To overcome such issues, augmentation operations have been carried out on the training set to boost the quantity of training images and prevent the overfitting problem that could arise when insufficient training data is employed. To accomplish such an objective, the original training images have been subjected to some transformations, including zoom, rotation, height shift, width shift, vertical flip, and horizontal flip, which produced new training samples for the training set. Random rotations of up to 360o have been implemented to images. Additionally, random zoom has been implemented in a factor of 0.20; shift of height and width in a factor of 0.20; random vertical and horizontal flips have been performed as well.

2.5. Hyper-parameter tuning

The performance of neural networks is significantly influenced by hyper-parameters such as the number of layers, optimization algorithm, learning rate, and activation functions. One of the most important problems facing every researcher in the field of neural network design is defining the hyperparameter since a misdescription of such parameters might result in an underfitting or overfitting model. VGG19 DL model was trained for this study, and the hyper-parameter was adjusted for optimal configuration. We trained multiple times using various hyper-parameter values to acquire appropriate results. Following several experiments, the Adam optimization technique was used in the model. For Adam, beta1 was equal to 0.9 and beta2 to 0.999. We employed 100 epochs and a learning rate of 0.001. For the model, the batch size was 32.

2.6. Evaluation criteria

Classification models frequently use metrics including sensitivity (recall), accuracy, precision, and specificity to evaluate their efficacy. A confusion matrix gives a thorough explanation of the classification results of certain samples. The comparison between the real and predicted labels for each image in the testing set is shown as a component of the confusion matrix. True positives (TP) represent the count of instances for which correct predictions were made. False negatives (FN) refer to the quantity

of instances which were incorrectly predicted. True negatives (TN) refer to the quantity of negative instances which were predicted correctly. False positives (FP) refer to the quantity of negative instances which were incorrectly predicted [18, 19].

Five criteria were used to assess the performance regarding the classification models:

Precision: proportion of all positive samples correctly forecasted to the total number of positive samples predicted [20].

$$precision = \frac{TP}{TP + FP} \tag{1}$$

Accuracy: The ratio of all samples properly predicted to all samples is known as accuracy[20].

$$Accuracy = \frac{TP + TN}{TP + FP + TN + FN} \tag{2}$$

Recall: Recall, also known as sensitivity, is the percentage of correctly classified positive samples in order to quantify the classifier's ability to correctly identify positive samples. The recall is expressed using the formula found in Equation (3). [21].

$$Recall = \frac{TP}{TP + FN} \tag{3}$$

F1-Score: Accuracy and recall in the classification task have a reciprocal relation. Although both qualities might be highly prized in an ideal scenario, the actual result is typically either great recall, yet low accuracy or low accuracy but high recall. F1-score is determined by averaging recall and accuracy harmonically. Equation (4) defines the F1-score. [22].

$$F1 - score = 2 * \frac{Precision * Recall}{Precision + Recall} \tag{4}$$

ROC: The ROC curve, short for receiver operating characteristic curve, shows how a parameter's specificity (false positive rate) and sensitivity (true positive rate) correlate at different thresholds. The area under curve (AUC) is the area under the ROC curve, which ranges from 0.1 to 1.0. AUC, being a numerical metric, enables a direct assessment of the classifier's quality. As AUC increases, so does the accuracy of classification. The AUC metric is not affected by the balance or imbalance of sample categories [23].

3. Results and Discussion

This section assesses the effectiveness of the suggested approach for classifying skin lesions. Specifically, we use five standardized metrics in medical image classification to quantitatively evaluate performance as well as classify the lesions from the HAM10000 dataset. Since the data set used consists of seven categories, the classification is multi-class, and in this way, we were able to calculate the recall, precision, F1_scoreand AUC values for each class for TL, FT for 5 executes.

Using a model which was trained on a specific dataset is known as transfer learning (TL). The model was re-used for solving other problems that were comparable to it by starting with it and update and change its parameters to meet the newly provided dataset. With the use of learning results from previous models, TL seeks to identify a model appropriate for the training dataset.The proposed model takes a dataset image with dimensions of 224×224×3 as input to the output of the probabilistic results from the last layer of the network. The VGG19 model was used by Including 3 fully-connected layers after that removed the last layer, Denes (1000) without fully connected classifier/layers, and adding a classifier skin disease Denes (7) as in Figure 3. It was the proposed model's overall accuracy (77.2±3.9623).

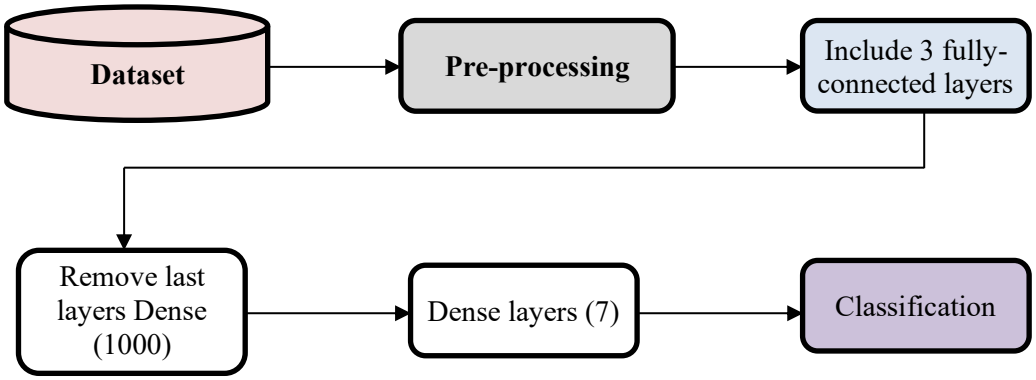

Figure 3. The architecture of the VGG19 model used

The goal of fine-tuning is to retain the knowledge acquired during the resolution of one problem and apply it to a different problem. By adjusting the weights regarding the top layers of pre-trained models, fine-tuning is an amazing technique to improve system performance. There are two approaches for fine-tuning: the first is setting the weight regarding specific layers to freeze. The number of resources and time required for fine-tuning decreases with the number of frozen layers. Alternatively, the entire architecture may be trained on a new database.

The VGG19 model was used, and we excluded 3 fully-connected layers. After that adding block: global average pooling 2D, Dense (256), Batch normalization layer, dropout (0.5), Dense (128), Batch normalization layer, dropout (0.5), Dense (64), and Batch normalization layer, after that add classifier Skin diseases Dense (7) As shown in figure 4 and a model has been produced, which has given a higher overall accuracy compared to the model that has been implemented in the transfer learning; it was (82.4±1.949359).

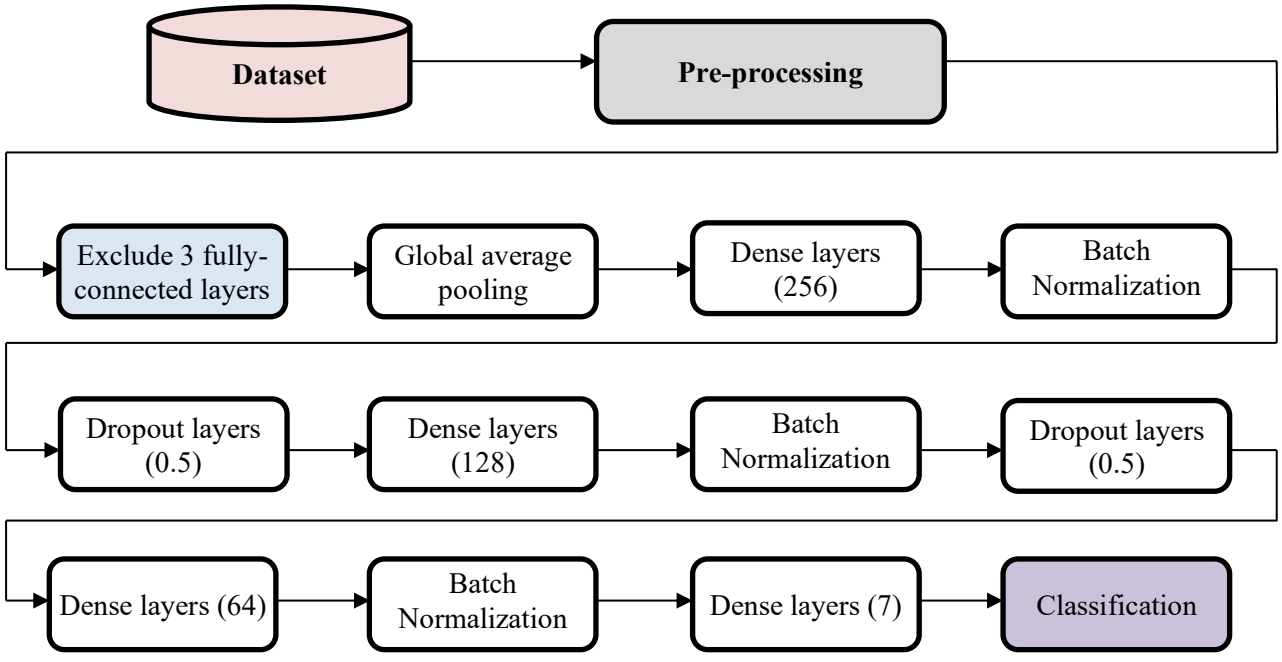

Figure 4. The architecture of the model proposed

After training the model for 60 epochs for the transfer learning method and 100 epochs for the fine-tuning method, the model's behavior was analyzed, as shown in Figures 5. Figure 6 presents ROC curves for (a) transfer learning and (b) fine-tuning. The horizontal axis measures the false positive rate, and the vertical axis measures the true positive rate. A higher AUC indicates better performance and improvement after fine-tuning.

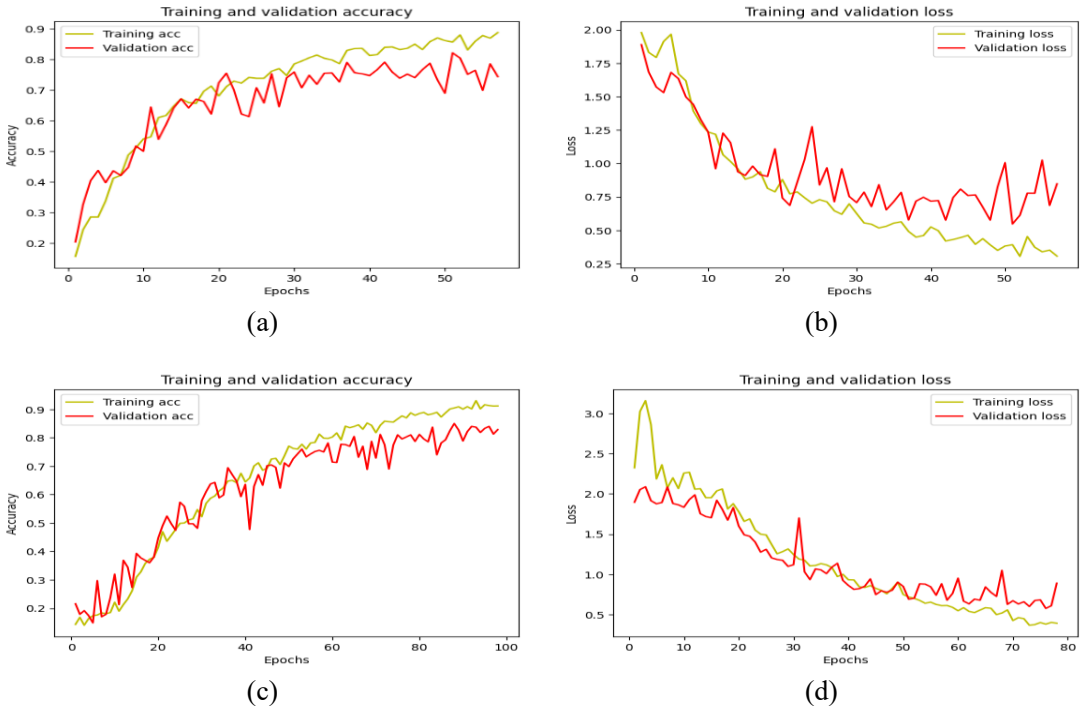

Figure 5. (a) Accuracy of transfer learning, (b) Loss of transfer learning, (c) Accuracy of Fine-tuning, (d) Loss of Fine-tuning

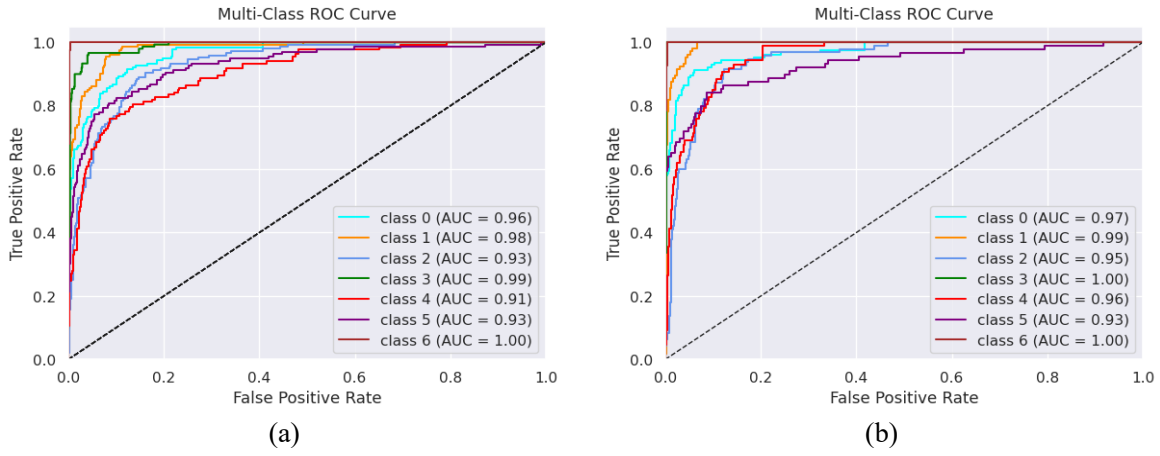

Figure 6. (a) ROC of transfer learning, (b) ROC of Fine-tuning

Figure 7 presents the confusion matrix for (a) transfer learning and (b) fine-tuning. The confusion matrix displays the true positives, true negatives, false positives, and false negatives, providing insight into the model's classification performance and error types. The model's performance was also evaluated based on the metrics for classification tasks performed, as shown in Table 2.

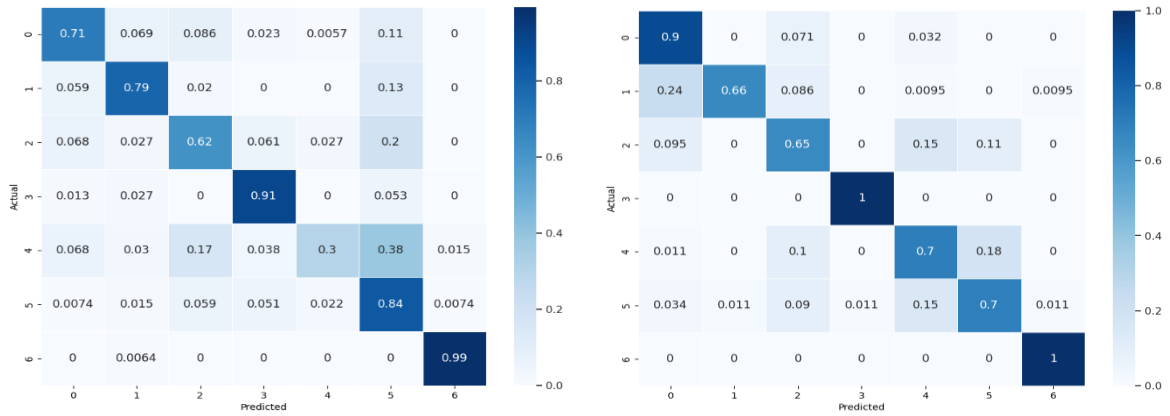

(a) (b)

Figure 7. The confusion matrix of (a) transfer learning, (b) Fine-tuning Systematics of the Article

Table 2. Results of transfer learning and Fine-tuning

Excute	Class	Transfer learning					Fine-tuning				
		Pres.	Rec.	F1	AUC	Acc.	Pres.	Rec.	F1	AUC	Acc.
1	0	0.80	0.71	0.75	0.96	0.74	0.75	0.90	0.82	0.97	0.81
	1	0.82	0.79	0.80	0.98		0.99	0.66	0.79	0.99	
	2	0.65	0.62	0.64	0.93		0.64	0.65	0.65	0.95	
	3	0.84	0.91	0.87	0.99		0.99	1.00	1.00	1.00	
	4	0.83	0.30	0.44	0.91		0.66	0.70	0.68	0.96	
	5	0.47	0.84	0.60	0.93		0.70	0.70	0.70	0.93	
	6	0.98	0.99	0.99	1.00		0.98	1.00	0.99	1.00	
2	0	0.89	0.73	0.80	0.98	0.82	0.96	0.78	0.86	0.96	0.83
	1	0.80	0.92	0.85	0.99		0.89	0.85	0.87	0.99	
	2	0.69	0.73	0.71	0.95		0.64	0.79	0.71	0.95	
	3	0.91	0.99	0.95	1.00		0.94	1.00	0.97	1.00	
	4	0.65	0.65	0.65	0.94		0.62	0.70	0.66	0.96	
	5	0.81	0.72	0.76	0.95		0.77	0.65	0.71	0.93	
	6	0.98	0.99	0.98	1.00		0.97	1.00	0.98	1.00	
3	0	0.74	0.90	0.81	0.98	0.81	0.89	0.77	0.83	0.95	0.83
	1	0.80	0.88	0.84	0.98		0.89	0.90	0.89	0.98	
	2	0.77	0.56	0.65	0.94		0.59	0.86	0.70	0.95	
	3	0.95	0.93	0.94	0.99		0.99	0.96	0.97	1.00	
	4	0.68	0.60	0.64	0.94		0.75	0.57	0.65	0.95	
	5	0.73	0.78	0.75	0.95		0.78	0.70	0.73	0.94	
	6	1.00	0.96	0.98	1.00		0.96	1.00	0.98	1.00	
4	0	0.90	0.52	0.66	0.94	0.75	0.87	0.86	0.86	0.97	0.85
	1	0.77	0.88	0.82	0.98		0.91	0.88	0.89	0.99	
	2	0.52	0.69	0.59	0.91		0.68	0.79	0.73	0.95	
	3	0.93	0.93	0.93	1.00		0.98	0.99	0.99	1.00	

	4	0.53	0.68	0.59	0.93		0.70	0.68	0.69	0.96	
	5	0.80	0.70	0.75	0.94		0.80	0.72	0.76	0.94	
	6	0.99	0.89	0.94	1.00		0.98	1.00	0.99	1.00	
5	0	0.78	0.79	0.79	0.96	0.74	0.83	0.65	0.73	0.96	0.80
	1	0.78	0.70	0.74	0.96		0.78	0.89	0.83	0.98	
	2	0.46	0.90	0.61	0.94		0.78	0.59	0.67	0.94	
	3	0.93	0.81	0.87	0.99		0.99	0.95	0.97	1.00	
	4	0.68	0.44	0.53	0.93		0.53	0.91	0.67	0.96	
	5	0.91	0.59	0.71	0.94		0.85	0.63	0.72	0.93	

4. Conclusion

One of the most common and dangerous malignancies is skin cancer. Dermatologists primarily use ocular diagnostics to diagnose this condition. Multiclass skin cancer classification is a challenging task because of the fine-grained variability in the appearance of its multiple diagnostic categories. However, in multiclass skin cancer classification, CNNs have surpassed dermatologists in recent studies. In order to support this endeavor, we resized every image to fit the requirements of each model and performed pretreatment steps such as data balance, data labeling, and data normalization. Using the HAM10000 dataset, we trained VGG19 by fine-tuning the CNNs and applying TL to pre-trained ImageNet weights. We assessed VGG19's performance on such multiclass classification tasks with the use of metrics like recall, precision, F1 Score, accuracy, and confusion matrices to examine the impact of TL and FT. The optimal performance was observed with FT. A number of factors, including the use of resolution scaling, image preprocessing, data augmentation, effective TL of ImageNet weight, and FT, contributed to the high classification results.

Acknowledgements

The authors would like to thank Mustansiriyah University for their valuable support and for providing essential facilities for this research.

References

[1] T. A. Putra, S. I. Rufaida, and J.-S. Leu, "Enhanced skin condition prediction through machine learning using dynamic training and testing augmentation," IEEE Access, vol. 8, pp. 40536-40546, 2020.

[2] T. Emara, H. M. Afify, F. H. Ismail, and A. E. Hassanien, "A modified inception-v4 for imbalanced skin cancer classification dataset," in 2019 14th International Conference on Computer Engineering and Systems (ICCES), 2019: IEEE, pp. 28-33.

[3] M. K. Hasan, M. A. Ahamad, C. H. Yap, and G. Yang, "A survey, review, and future trends of skin lesion segmentation and classification," Computers in Biology and Medicine, p. 106624, 2023.

[4] H. K. Gajera, D. R. Nayak, and M. A. Zaveri, "A comprehensive analysis of dermoscopy images for melanoma detection via deep CNN features," Biomedical Signal Processing and Control, vol. 79, p. 104186, 2023/01/01/ 2023, doi: https://doi.org/10.1016/j.bspc.2022.104186.

[5] M. Y. Kamil and A. A. Jassam, "Analysis of Tissue Abnormality in Mammography Images Using Gray Level Co-occurrence Matrix Method," *Journal of Physics: Conference Series*, 2020, Vol. 1530, 012101, doi: 10.1088/1742-6596/1530/1/012101.

[6] N. F. Lattoofi, I. F. Al-Sharuee, M. Y. Kamil, A. H. Obaid, A. A. Mahidi, A. A. Omar, and A. K. Saleh, "Melanoma Skin Cancer Detection Based on ABCD Rule," in 1st International Scientific Conference of Computer and Applied Sciences, CAS 2019, 2019, pp. 154-157, doi: 10.1109/CAS47993.2019.9075465.

[7] M. A. Al-Masni, D.-H. Kim, and T.-S. Kim, "Multiple skin lesions diagnostics via integrated deep convolutional networks for segmentation and classification," Computer methods and programs in biomedicine, vol. 190, p. 105351, 2020.
[8] M. A. Shames and M. Y. Kamil, "Development and Validation of a Diagnosis System for Lung Infection Using Hybrid Deep-Learning Techniques," Journal of Studies in Science and Engineering, Article vol. 4, no. 1, pp. 61-74, 2024, doi: 10.53898/josse2024415.
[9] Z. Qin, Z. Liu, P. Zhu, and Y. Xue, "A GAN-based image synthesis method for skin lesion classification," Computer Methods and Programs in Biomedicine, vol. 195, p. 105568, 2020.
[10] A. Mahbod, G. Schaefer, C. Wang, G. Dorffner, R. Ecker, and I. Ellinger, "Transfer learning using a multi-scale and multi-network ensemble for skin lesion classification," Computer methods and programs in biomedicine, vol. 193, p. 105475, 2020.
[11] M. S. Ali, M. S. Miah, J. Haque, M. M. Rahman, and M. K. Islam, "An enhanced technique of skin cancer classification using deep convolutional neural network with transfer learning models," Machine Learning with Applications, vol. 5, p. 100036, 2021.
[12] I. Iqbal, M. Younus, K. Walayat, M. U. Kakar, and J. Ma, "Automated multi-class classification of skin lesions through deep convolutional neural network with dermoscopic images," Computerized medical imaging and graphics, vol. 88, p. 101843, 2021.
[13] M. A. Khan, Y.-D. Zhang, M. Sharif, and T. Akram, "Pixels to classes: intelligent learning framework for multiclass skin lesion localization and classification," Computers & Electrical Engineering, vol. 90, p. 106956, 2021.
[14] M. A. Shames and M. Y. Kamil, "Early Diagnosis of Lung Infection via Deep Learning Approach," International Research Journal of Multidisciplinary Technovation, Article vol. 6, no. 3, pp. 216-224, 2024, doi: 10.54392/irjmt24316.
[15] A. Bhola, S. Verma, and P. Kumar, "A comparative analysis of deep learning models for cucumber disease classification using transfer learning," Journal of Current Science and Technology, vol. 13, no. 1, pp. 23-35, 2023.
[16] L. Sushma and K. Lakshmi, "An analysis of convolution neural network for image classification using different models," Int J Eng Res Technol (IJERT), vol. 9, no. 10, 2020.
[17] H. S. Ibrahim, N. M. Shati, and A. A. Alsewari, “A Transfer Learning Approach for Arabic Image Captions”, Al-Mustansiriyah Journal of Science, vol. 35, no. 3, 2024. pp. 81–90, doi: 10.23851/mjs.v35i3.1485.
[18] U. Khasanah, B. Surarso, and F. Farikhin, "Dilated Convolutional Neural Network for Skin Cancer Classification Based on Image Data," JTAM (Jurnal Teori dan Aplikasi Matematika), vol. 7, no. 1, pp. 196-207, 2023.
[19] R. R. Kadhim and M. Y. Kamil, "Comparison of breast cancer classification models on Wisconsin dataset," International Journal of Reconfigurable and Embedded Systems, Article vol. 11, no. 2, pp. 166-174, 2022, doi: 10.11591/ijres.v11.i2.pp166-174.
[20] M. M. Chowdhury, R. S. Ayon, and M. S. Hossain, "An investigation of machine learning algorithms and data augmentation techniques for diabetes diagnosis using class imbalanced BRFSS dataset," Healthcare Analytics, p. 100297, 2023.
[21] A. H. Barshooi and A. Amirkhani, "A novel data augmentation based on Gabor filter and convolutional deep learning for improving the classification of COVID-19 chest X-Ray images," Biomedical Signal Processing and Control, vol. 72, p. 103326, 2022.
[22] X. Cao, J.-S. Pan, Z. Wang, Z. Sun, A. ul Haq, W. Deng, and S. Yang, "Application of generated mask method based on Mask R-CNN in classification and detection of melanoma," Computer Methods and Programs in Biomedicine, vol. 207, p. 106174, 2021.
[23] S. H. Mousa, N. M. Shati, and N. Sakthivadivel, "DeepRing: Convolution Neural Network based on Blockchain Technology," Al-Mustansiriyah Journal of Science, vol. 35, no. 2, pp. 61-69, 2024, doi: 10.23851/mjs.v35i2.1476.